Mechanics & Industry 15, 307–312 (2014)

DOI: 10.1051/meca/2014037
www.mechanics-industry.org

Mechanics & Industry

Local thermal characterization of metal sample by stimulated infra-red thermography

K. Mouhoubi[a], J.L. Bodnar, S. Ousseni, J.L. Nicolas and D. Caron

GRESPI/ECATHERM, UFR Exact sciences and Natural, BP 1039, 51687 Rheims Cedex 02, France

Received 7 January 2014, Accepted 15 May 2014

Abstract – In this paper, we consider the possibilities of the stimulated infra-red thermography for local metallic sample thermal characterization. At first we introduce the measurement principle, which is based on the local measurement of the thermal diffusivity parameter. Then, using simulations, we demonstrate the feasibility of the method. We then present the experimental device implemented for the study. Finally, we show that this approach allows a good estimation of the thermal diffusivity of a metal sample.

Key words: Non destructive testing / thermal characterization / metallic sample / iron / stimulated infrared thermography / thermal diffusivity measurement

1 Introduction

The non destructive testing of the samples is being used more and more in the industrial field. The aim of this type of control is to offer to the customers machined parts providing the best possible quality. Many NDT techniques are also further implemented to follow the ageing of industrial materials. Without being exhaustive, we can quote the ultrasounds, the Eddy's currents, the penetrant testing method, the magnetic particle inspection, the X and γ radiography and the visual monitoring [1,2]. Other techniques, such as those using the thermal waves, start to develop. Here we can quote the stimulated infrared thermography implemented in our study. This method has the advantage of being without contact, of being able to be applied remotely and finally of being very flexible [3–25]. In addition, the cost of the equipment decreases while the materials become increasingly powerful. Therefore it seemed interesting to us to consider the possibilities of this particular method for the local thermal characterization of metal samples. This type of measurement is indeed necessary in order to for example: determine the depth of a defect, estimate a thickness of coating or appreciate a loss of thickness related to corrosion. The approach presented in this work aims at considering the thermal diffusivity of the sample studied starting from a local laser excitation and of a spatio-temporal analysis of the photothermal answer then obtained. Our presentation breaks up into four parts. In the first place, we introduce the principle of the method of measurement. Second, using simulations, we demonstrate the feasibility of the method. We then present the experimental device implemented for the study. Finally, we show that the approach allows a good estimate of the local thermal diffusivity of sample chromium-nickel-steel.

2 Principle of the measurement method used

The principle of the method of local estimate of thermal diffusivity retained for the study is the following: an anisotropic sample is subjected on its front face to an excitation temporally close to a function delta of Dirac $\delta(t)$ and space form $f(x,y)$ unspecified. Then, using an infrared camera of thermography, we measure the field of surface temperature of the studied sample. From the temporal evolution of this field of temperature, we go up, using a post mathematical treatment, the values of thermal diffusivity of material according to its directions of anisotropy. Let us examine in details this mathematical post-treatment on which this measurement technique is based. λ_x, λ_y and λ_z are the thermal conductivities of the studied sample. These thermal conductivities will be supposed to be constant in time and according to the temperature (assumptions of short analysis and weak temperature variations). ρ and Cp stand for the density and the heat-storage capacity of this same sample. a_x, a_y and a_z represent the thermal diffusivities of the studied sample. h_0 and he are the exchange coefficients of the front and back faces of the sample. e is the thickness of the studied sample. This thickness is supposed very weak in front of side dimensions of the sample, which makes it possible

[a] Corresponding author: kamel.mouhoubi@univ-reims.fr

$$\Theta(\alpha_n,\beta_m,z=0,p)=\frac{F(\alpha_n,\beta_m)(\mathrm{ch}(\gamma_{n,m}e)+h_e\mathrm{sh}(\gamma_{n,m}e)/(\lambda_z\gamma_{n,m}))}{\lambda_z\gamma_{n,m}\mathrm{sh}(\gamma_{n,m}e)+(h_0+h_e)\mathrm{ch}(\gamma_{n,m}e)+h_0h_e\mathrm{sh}(\gamma_{n,m}e)/(\lambda_z\gamma_{n,m})} \quad (3)$$

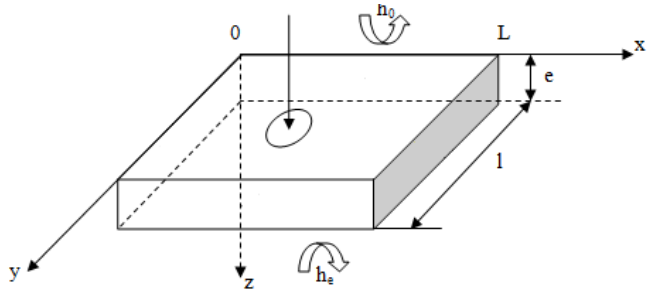

Fig. 1. Boundary conditions retained for the study.

to neglect the side convecto-radiative losses of the sample. Finally, the sample is considered initially in thermal balance with its environment (Fig. 1).

The mathematical translation of these assumptions leads to the following differential system:

$$\begin{aligned}
&\lambda_x(\partial^2T/\partial x^2)+\lambda_y(\partial^2T/\partial y^2)+\lambda_z(\partial^2T/\partial z^2)=\rho c(\partial T/\partial t)\\
&\text{At } z=0\ \lambda_z(\partial T/\partial z)_{z=0}=h_0(T(z=0)-T_{\mathrm{ext}})-f(x,y)\delta(t)\\
&\text{At } z=e \qquad \lambda_z(\partial T/\partial z)_{z=0}=-h_e(T(z=e)-T_{\mathrm{ext}})\\
&\text{At } x=0 \quad \text{et} \quad x=L_{\mathrm{x}}, \qquad \partial T/\partial x=0\\
&\text{At } y=0 \quad \text{et} \quad y=L_{\mathrm{y}}, \qquad \partial T/\partial y=0\\
&\text{At } t=0, \qquad T=T_{\mathrm{ext}}
\end{aligned} \quad (1)$$

To solve this differential connection, we chose to implement three integral transformations; a transformation of Laplace into time associated with a transformation of Fourier into a cosine that coordinates with space X and there:

$$\Theta(\alpha_n,\beta_m,z,p)=\int_{t=0}^{\infty}\int_{y=0}^{L_y}\int_{x=0}^{L_x}T(x,y,z,t)\cos(\alpha_n x)\times\cos(\beta_m y)\exp(-pt)\mathrm{d}x\mathrm{d}y\mathrm{d}t \quad (2)$$

with:

- $\alpha_{\mathrm{n}}=n\pi/L_x$;
- $\beta_{\mathrm{m}}=m\pi/L_{\mathrm{y}}$.

By applying this integral transformation to the preceding differential connection, the differential equation to solve in space transformed does not depend any more that of Z and can thus be solved easily by the method of the thermal quadrupoles [26]. We then obtain:

See equation (3) above

with:

– $\gamma_{n,m}=\sqrt{p/a_z+(\lambda_x/\lambda_z)\alpha_n^2+(\lambda_y/\lambda_z)\beta_m^2}$;
– $F(\alpha n,\beta m)$, the transform of Laplace Fourier of exiting flow $f(x,y)\,\delta(t)$.

Now taking the opposite transform of Laplace of the temperature, we gain:

$$\mathrm{Ln}\left(\frac{\theta(\alpha_n,\beta_m,z=0,t)}{\theta(0,0,z=0,t)}\right)=\mathrm{Ln}\left(\frac{F(\alpha_n,\beta_m)}{(F(0,0))}\right)-\left(a_x\alpha_n^2t+a_y\beta_m^2t\right) \quad (4)$$

It is noticed whereas longitudinal diffusivities ax and ay can be deduced simply from the slope of the curve representing the report/ratio of the logarithm of the coefficients of Fourier traced compared to time (5).

$$a=\frac{Slope\_of\_the\_curve\times Dimension\_of\_the\_area^2}{Fourier's\_order^2\times\pi^2} \quad (5)$$

3 Theoretical study

Initially, in order to approach the feasibility of the method, we developed a theoretical study based on numerical simulations. We implemented the finite element method to solve the preceding differential system. The sample that we studied is a cylinder of chromium-nickel steel (18 Cr, 8 Ni) 30 mm in diameter and 10 mm thick. The thermo-physical properties taken into account are the following. The thermal conductivity is equal to 14.3 W.m^{-1}.K. The heat capacity is equal to 460 J.kg^{-1}.K. The density is equal to 7820 kg.m^{-3}. Thus, thermal diffusivity is equal to 3.98×10^{-6} m.s^{-1}. The excitation flash was imposed on the centre of the sample and its duration is equal to 20 ms. Its characteristic diameter is equal to 1.8 mm. The deposited power is equal to 3 W. Convective exchanges are considered on the upper and lower faces of the sample. The value of the coefficient of exchange is equal to 10 W.m^{-2}.K^{-1}. In order to reduce the computing times, a progressive grid of the sample was considered. This grid retained finer on the level of the excited zone and coarser on the edges of the sample (Fig. 2). Elementary space dimension is equal to 200 μm. The step of computing time is equal to 2 ms. The duration of observation is equal to 0.8 s.

In order to lead up to the theoretical measurement of longitudinal thermal diffusivity, we initially calculated for each step in time the thermal signature on the surface of the studied sample. Figures 3 and 4 show that this very intense and localized signature becomes less full and wider with time.

For each obtained thermogram, we then calculated the average in a direction of space in order to consider diffusivity thermal in the perpendicular direction. We further broke up the result obtained in the space of Fourier using a transformation into a cosine. Finally, we calculated the temporal evolution of the report/ratio of the coefficients of Fourier to order 2, compared to the coefficient of

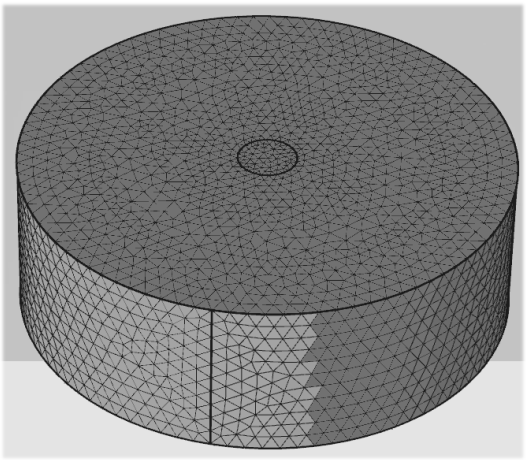

Fig. 2. Grid used for the study.

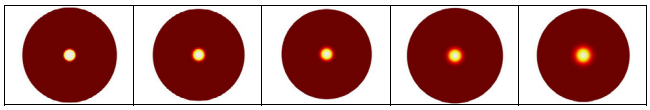

Fig. 3. Evolution of the thermal signature of the sample studied with time (respectively $t = 20$ ms; $t = 40$ ms; $t = 60$ ms; $t = 100$ ms and finally $t = 200$ ms).

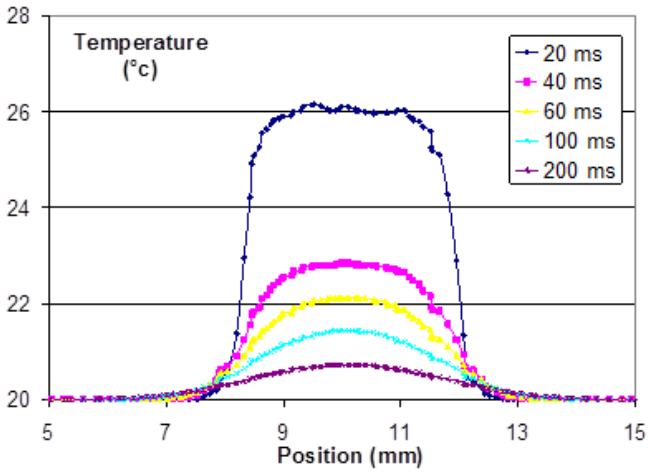

Fig. 4. Evolution of the central profiles of the thermal signature of the sample studied with time (respectively $t = 20$ ms; $t = 40$ ms; $t = 60$ ms; $t = 100$ ms and finally $t = 200$ ms).

Fourier calculated with order 0. In Figure 5, we present the result obtained. As predicted, it reveals a line with a negative slope. We then analyzed this slope in order to conclude a required thermal diffusivity. We found a value of $-1.54\ \mathrm{s}^{-1}$. As the width of the analyzed zone is of 1 cm, formula (5) leads to a value of thermal diffusivity equal to $3.92 \times 10^{-6}\ \mathrm{m}^2.\mathrm{s}^{-1}$. This value is very close, except for the numerical errors with the theoretical value equal to $3.98 \times 10^{-6}\ \mathrm{m}^2.\mathrm{s}^{-1}$. This seems to show the theoretical feasibility of the method.

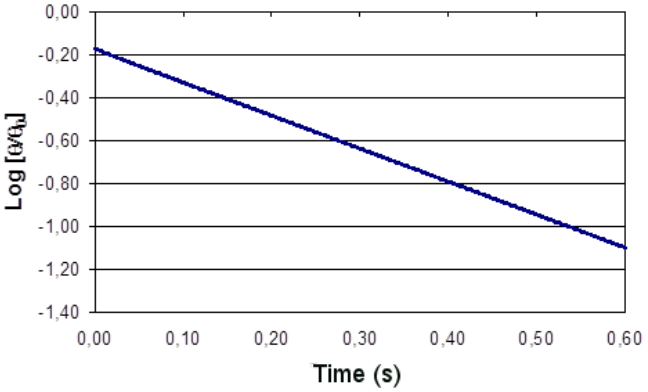

Fig. 5. Temporal evolution of the report/ratio of the coefficients of Fourier with order 2 and order 0.

4 The experimental device implemented for the study

After the encouraging results of the theoretical study, we decided to develop an experimental study in order to try to confirm them. The device implemented is presented in Figure 6. It shows that the excitation is provided by a laser diode. The later is controlled electronically while running, with a wavelength of emission of 0.808 μm and maximum power of 4 W. This source of light is placed on a horizontal support, aiming at a mirror of reference which allows a quasi normal excitation of the studied sample. The type of excitation implemented during the study is impulse. The duration of excitation corresponded to 20 ms. Finally, the characteristic diameter of the spot of excitation is of approximately 2 mm. Figure 6 also demonstrates that the detection of the photothermal signal is ensured by an infra-red camera of thermography. As the duration of the thermal transient used for the study is close to several hundred milliseconds, it is a bolometer camera. On one side such a camera is slower but on the other much less expensive than a matrix camera of quantum detectors. With a view of technology transfer in mind, it can be bought more easily by the industrialists, which further justifies our choice. In addition, because of the heating being rather limited, we chose a "long wave" camera, which is more adapted for the study of the temperatures close to the ambient one. Lastly, to obtain a sufficient space resolution, our equipment also included an A20 camera with Flir, an objective of macrothermography. It allows a side space resolution of approximately 100 μm. This system of detection is placed perpendicular to the sample at a distance of approximately 20 cm. In order to have a sufficient temporal resolution, we fixed the frequency of acquisition of the infra-red camera thermography at 50 Hz.

5 The studied sample

The studied sample in our experiment was a pastille of steel-nickel-chromium, 30 mm in diameter and 10.21 mm

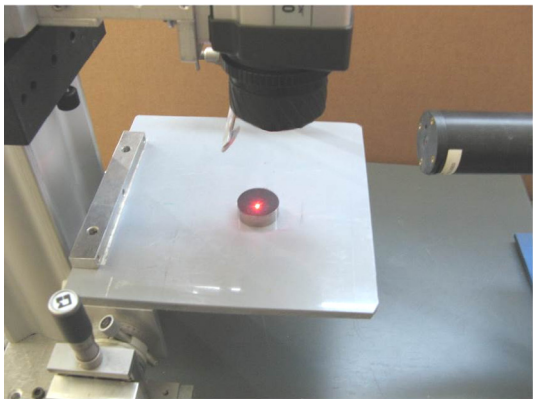

Fig. 6. The experimental device implemented for the study.

Fig. 7. The studied sample.

thick. It was covered with a fine coat of black paint in order to improve and to homogenize its radiative properties (Fig. 7).

In order to obtain a thermal value of diffusivity of reference, this sample was initially studied with the diffusivimeter flash with contact of reference of the laboratory. It is a system allowing a precise measurement of the thermal parameter diffusivity by a photothermal analysis back face and with contact. As presented in Figure 8, the composition of the system of excitation is made up of 4 flash lamps. It is fed by a source of a tension of 1000 V, allowing a deposit of energy during approximately 5 ms on the front face of the analyzed sample. The temperature measurement is ensured by a thermocouple contact separated out of Bismuth telluride (Bi_2Te_3), which comes in electrical contact from the back face of the analyzed sample. The device is supplemented by a software continuation allowing a measurement of the thermal parameter diffusivity by 4 methods of examinations: method of Parker (method without losses), method of part times, method of the moments and finally an adjustment theory/experiment [27,28].

The result obtained during the analysis of our sample is presented in Figure 9. It shows that the thermal diffusivity of our sample is evaluated 4.14×10^{-6} $m^2.s^{-1}$ with the method of Parker, 4.07×10^{-6} $m^2.s^{-1}$ with the method of part times, 4.00×10^{-6} $m^2.s^{-1}$ with the method of the moments and 4.12×10^{-6} $m^2.s^{-1}$ with the adjustment theory/experiment.

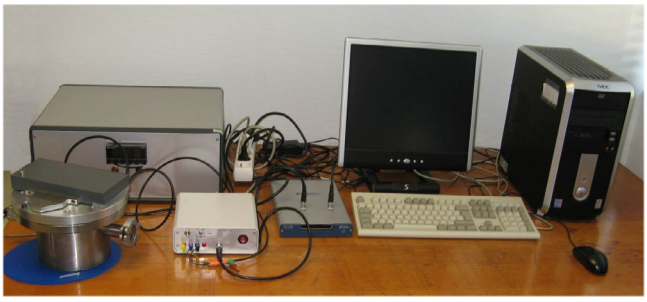

Fig. 8. The diffusivimeter with contact of laboratory used.

6 Experimental results obtained by photothermal analysis front face

The front face of the sample was then analyzed with the help of a stimulated infra-red thermography. The center part surface of this sample was enlightened at approximately 12.5 mm, with a power of 3 W and during 20 ms. This heating was recorded synchronously with the excitation by an infrared camera of thermography. It is a Flir A20 type in macro mode. Figures 10 and 11 present the temporal evolution of the thermal signature of the obtained laser spot. They show, as we have anticipated in the theory, the signatures becoming wider and less intense with time.

As during the theoretical simulations and as the theory envisaged it, we then calculated the average of these images in a direction of space and taken the transforms as a cosine of the results obtained. For each various image we calculated the logarithm of the report/ratio of the coefficients of Fourier obtained with order 2 and order 0. Figure 12 represents these results and revealing, just like the theory foretold, a line with a negative slope. It is equal, in this case to -7.77 s^{-1}.

We finished our experiment with a measurement of longitudinal diffusivity by calibrating spatially our experimental device. For that, we placed a standard hold on the surface of the studied and deduced object, infra-red image obtained, the space dimension seen by pixel. We found a value of 115 μm. Formula (5) has then allowed us to determine the longitudinal value of the thermal diffusivity of the analyzed steel sample. We find a median value equal to 4.06×10^{-6} $m^2.s^{-1}$. This value is very close to those gained classically with the flash method, which seems to show the possibilities of the method as regards measurement "in situ", of this thermophysical parameter.

7 Conclusion

In this work, we considered the possibilities of the infra-red thermography stimulated as regards thermal characterization in situ, of metal sample. We introduced the principle of the measurement method. We demonstrated the feasibility of the method using digital simulation.

We presented the experimental device implemented for the study. We showed, using the experimental study

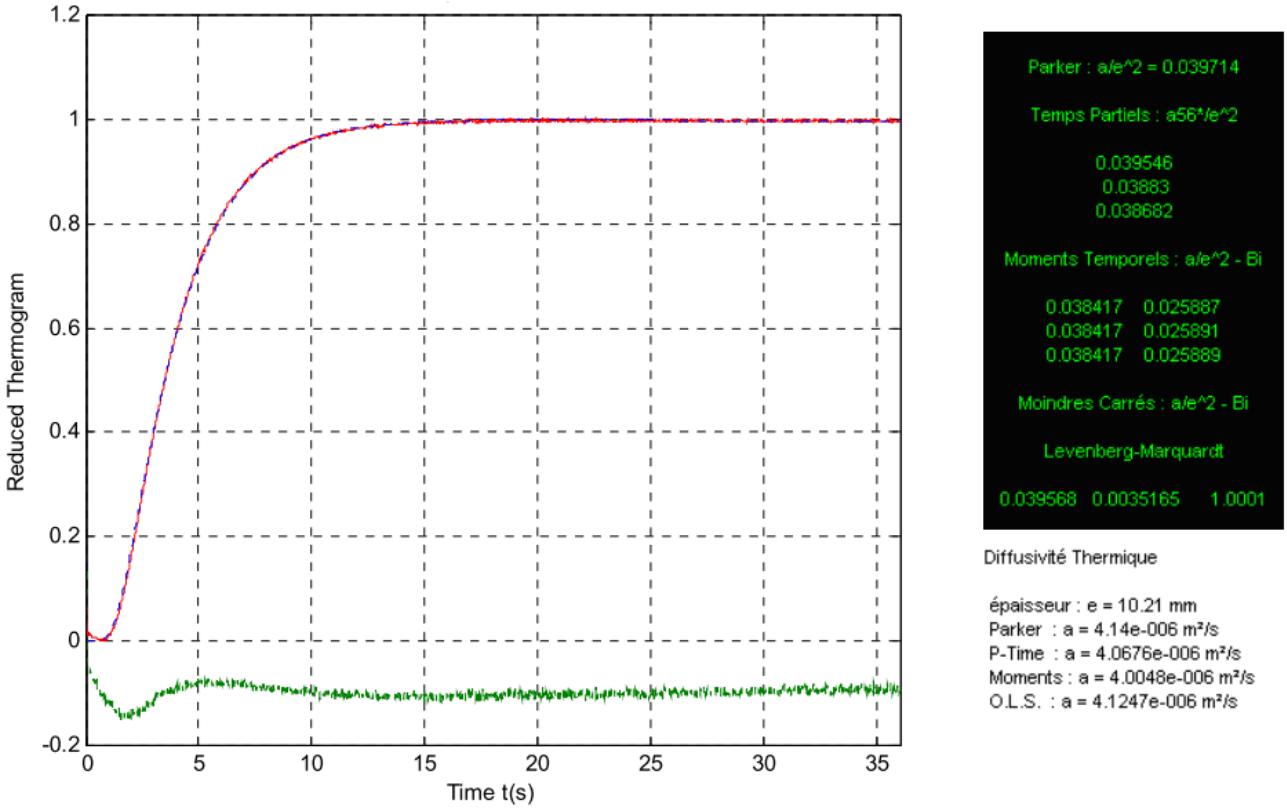

Fig. 9. Measure thermal diffusivity of the sample assistance of a diffusivimeter flash of laboratory.

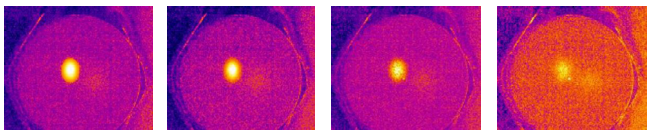

Fig. 10. Evolution of the infra-red signature of the laser heating with time (respectively with $t = 20$ ms, $t = 40$ ms, $t = 80$ ms and $t = 200$ ms).

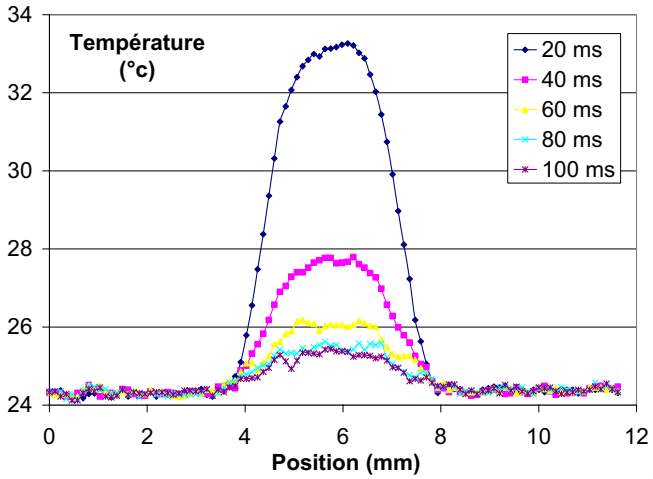

Fig. 11. Evolution of the central profiles of the infra-red signature of the laser heating with time (respectively with $t = 20$ ms, $t = 40$ ms, $t = 80$ ms and $t = 200$ ms).

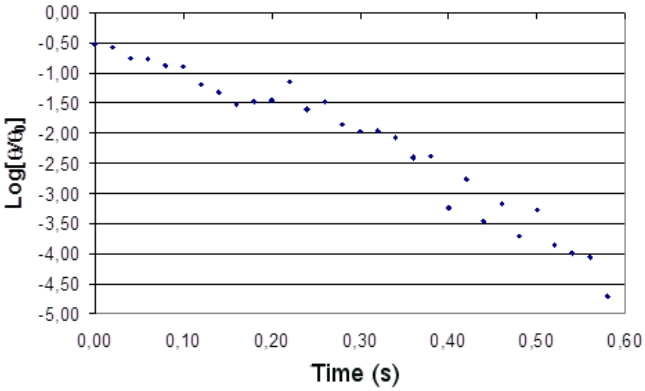

Fig. 12. Evolution of the report/ratio of the logarithms of the coefficients of Fourier, calculated with the order 2, calculated for each infra-red image according to time.

of a steel sample chromium plates nickel, that the photothermal method allows, in a particular case, a good approximation of the thermal parameter diffusivity. This experimental result, gained from a particular sample, is encouraging since pretense to open the way with the photothermal metallic material characterization in situ. The question at hand is if these results can be generalized. In addition, more conclusions have to be made about the possibility to use tools for geometrical characterization, to lead industrially to measurements of depth of inclusion,

with thickness measurements of coating or in die of thickness loss of matter related to corrosion. Studies dealing with these issues are being conducted.

References

[1] J. Dumont-Fillon, Contrôle non destructif, Techniques de l'ingénieur R1400 (2013) 9–54

[2] M. Cherfaoui, Essais non destructifs, Techniques de l'ingénieur R1400 (2013) 55–68

[3] C. Joseph, L'observation et le mesurage par thermographie infrarouge

[4] C. Joseph, Passive infrared detection

[5] G. Gilbert, La thermographie infrarouge : Principes, technologies, applications

[6] M. Xavier, Theory and practice of infrared technology for non destructive testing

[7] M. Andreas, Progress in Photothermal and Photoacoustic Sciences and Technology

[8] P. Dominique, Mesure par thermographie infrarouge

[9] P. François, G. Paulin, Thermographie infrarouge : Images et mesure

[10] V.P. Vavilov, Non destructive testing handbook: thermal/infrared testing

[11] H.G. Walther, D. Fournier, J.C. Krapez, M. Luukkala, B. Schmitz, C. Sibilia, H. Stamm, J. Thoen, Photothermal Steel Hardness Measurements – Results and Perspectives, Anal. Sci. 17 (2001) s158–s160

[12] Th. Zweschper, A. Dillenz, G. Riegert, D. Scherling, G. Busse, Ultrasound excited thermography using frequency modulated elastic waves, Insight 45 (2003) 178–182

[13] J. Vrana, M. Goldammer, J. Baumann, M. Rothenfusser, W. Arnold, Mechanisms and Models for Crack Detection with Induction Thermography, Review of Progress in QNDE 27 (2008) 475–482

[14] H. Mooshofer, M. Goldammer, W. Heine, M. Rothenfusser, J. Bass, E. Lombardo, J. Vrana, Induktionsthermographie zur automatischen Prüfung von Generatorkomponenten, DGZfP-Jahrestagung 2009, Münster (Allemagne), 2009

[15] J. Bamberg, G. Erbeck, G. Zenzinger, EddyTherm: Ein Verfahren zur bildgebenden Rißprüfung metallischer Bauteile, ZfP-Zeitung 68 (1999) 60−62

[16] G. Riegert, Th. Zweschper, A. Dillenz, G. Busse, Wirbelstromangeregte Lockin-Thermografie – Prinzip und Anwendungen, DACH – Jahrestagung 2004 Salzburg

[17] J.L. Bodnar, M. Edée, Wear characterization by photothermal radiometry, Wear 196 (1996) 54–59

[18] J.L. Bodnar, M. Edée, C. Menu, R. Besnard, A. Le Blanc, M. Pigeon, J.Y. Sellier, Cracks detection by a moving photothermal probe, J. Phys. IV 4 (1994) C7-591

[19] J.C. Candoré, J.J. Bodnar, V. Detalle, P. Grossel, Non-destructive testing of works of art by stimulated infrared thermography, EPJ Appl. Phys. 57 (2012) 21002

[20] J.C. Candoré, J.L. Bodnar, V. Detalle, P. Grossel, Characterization of defects situated in a fresco by stimulated infrared thermography, EPJ Appl. Phys. 57 (2012) 11002

[21] J.L Bodnar, J.C Candoré, J.L. Nicolas, G. Szatanik, V. Detalle, J.M. Vallet, Stimulated infrared thermography applied to help restoring mural paintings NDT and E International 49 (2012) 40–46

[22] S. Maillard, J. Cadith, P. Bouteille, G. Legros, J.L. Bodnar, V. Detalle, Non destructive testing of forged metallic materials by active infrared thermography, Int. J. Thermophys. 33 (2012) 1982–1988

[23] J.L. Bodnar, J.L. Nicolas, J.C. Candoré, V. Detalle, Non-destructive testing by infrared thermography under random excitation and ARMA analysis, Int. J. Thermophys. 33 (2012) 2011–2015

[24] J.L. Bodnar, K. Mouhoubi, G. Szatanik-Perrier, J.M. Vallet, V. Detalle, Photothermal thermography applied to the non-destructive testing of different types of works of art, Int. J. Thermophys. 33 (2012) 996–2000

[25] J.L. Bodnar, S. Brahim, P. Grossel, V. Detalle, Rear face photothermal analysis under random excitation and parametric analysis: Application to thermal diffusivity measurement, Int. J. Thermophys. 33 (2012) 1976–1981

[26] D. Maillet, S. André, J.C. Batsale, A. Degiovanni, C. Moyne, Thermal quadrupoles, Wiley

[27] W.J. Parker, R.J. Jenkins, C.P. Butler, G.L. abbott, Flash method of determining thermal diffusivity, heat capacity and thermal conductivity. J. Appl. Phys. 32 (1961) 1679–1684

[28] J. Hladik, Métrologie des propriétés thermophysiques des matériaux, Masson, 1990